View metadata, citation and similar papers at core.ac.uk

brought to you by CORE

provided by University of Birmingham Research Portal

UNIVERSITY OF BIRMINGHAM

Research at Birmingham

Sol-gel synthesis and formation mechanism of ultrahigh temperature ceramic

Venugopal, Saranya; Boakye, Emmanuel E.; Paul, Anish; Keller, Kristin; Mogilevsky, Pavel; Vaidhyanathan, Bala; Binner, Jon; Katz, Allan; Brown, Peter M.

DOI:
10.1111/jace.12654

License:
Unspecified

Document Version
Peer reviewed version

Citation for published version (Harvard):
Venugopal, S, Boakye, EE, Paul, A, Keller, K, Mogilevsky, P, Vaidhyanathan, B, Binner, JGP, Katz, A & Brown, PM 2014, 'Sol-gel synthesis and formation mechanism of ultrahigh temperature ceramic: HfB2', Journal of the American Ceramic Society, vol. 97, no. 1, pp. 92-99. https://doi.org/10.1111/jace.12654

Link to publication on Research at Birmingham portal

General rights
Unless a licence is specified above, all rights (including copyright and moral rights) in this document are retained by the authors and/or the copyright holders. The express permission of the copyright holder must be obtained for any use of this material other than for purposes permitted by law.

- Users may freely distribute the URL that is used to identify this publication.
- Users may download and/or print one copy of the publication from the University of Birmingham research portal for the purpose of private study or non-commercial research.
- User may use extracts from the document in line with the concept of ‘fair dealing’ under the Copyright, Designs and Patents Act 1988 (?)
- Users may not further distribute the material nor use it for the purposes of commercial gain.

Where a licence is displayed above, please note the terms and conditions of the licence govern your use of this document.

When citing, please reference the published version.

Take down policy
While the University of Birmingham exercises care and attention in making items available there are rare occasions when an item has been uploaded in error or has been deemed to be commercially or otherwise sensitive.

If you believe that this is the case for this document, please contact UBIRA@lists.bham.ac.uk providing details and we will remove access to the work immediately and investigate.

Download date: 01. Feb. 2019

Low Temperature Synthesis and Formation Mechanism of HfB_2 Powder

Venugopal S[ai], Boakye EE[b], Paul A[a], Keller K[b], Mogilevsky P[b], Vaidhyanathan B[a], Binner JGP[a], Katz A[b] and Brown PM[c].

[a]Department of Materials, Loughborough University, UK, LE11 3TU

[b]Wright Patterson AFB, Dayton, Ohio, USA, 45433

[c]DSTL, Porton Down, Salisbury, UK, SP4 0JQ

Abstract

HfB_2 is an ultra-high temperature ceramic that holds great potential for use in thermal protection systems because of favourable temperature stability, good mechanical properties and oxidation resistance. In this work HfB_2 powder has been synthesised via a sol-gel based route using phenolic resin, hafnium chloride and boric acid as the source of carbon, hafnium and boron respectively, though a small number of comparative experiments involved amorphous boron as boron source. The effects of calcination dwell time and Hf:C and Hf:B molar ratio on the purity and morphology of the final powder have been studied and the mechanism of HfB_2 formation investigated using FTIR, TGA, DSC and XRD. The results showed that whilst temperatures as low as 1300°C could be used to produce HfB_2 particles, the calcination needed to last for about 25 h and the long duration resulted in particle growth along the c-axis of the HfB_2 crystals yielding tube like structures of about 10 µm long. Equiaxed particles 1 – 2 µm in size were obtained when the precursor was calcined at 1600°C for 2 h. The reaction mechanism involved carbo/borothermal reduction and the indications were that the formation of HfB_2 at 1300°C is through

---

[i] Corresponding author at: Department of Materials, Loughborough University, Loughborough, Leicestershire LE11 3TU, UK. Tel.: +44 1509223154; fax: +44 1509223949. E-mail address: S.Venugopal@lboro.ac.uk (S. Venugopal).

the intermediate formation of an amorphous B or boron sub oxides, although at higher temperatures more than one reaction mechanism may be active.

Keywords: Ultra-high temperature ceramics, HfB_2, sol gel, reaction mechanism.

1. Introduction

Many exotic materials such as Inconel x/x-750, Ti-Zr-Mo alloys, Cf-SiC composites, taz-8a cermets, Ti metal matrix composites and ultra-high temperature ceramics based on the borides and carbides have been created since the 1960s to be used as the wing leading edge and propulsion components in hypersonic vehicles in order to withstand temperatures in excess of 2000^{o}C and to offer ablation resistance [1]. Hafnium diboride (HfB_2) has a hexagonal AlB_2-type layered structure with B atoms in 2D graphite-like rings and alternate hexagonally close-packed Hf layers [2]. The strong Hf-B and B-B bonds are responsible for the very high melting point of 3250^{o}C, high oxidation resistance and high hardness of about 29±5 GPa, whilst the electron concentration around the boron gives rise to electrical conductivity in the material [2]. Due to these properties, HfB_2 has several commercial and lab scale applications including electron emitters, catalysts, cutting tools, rocket nozzle inserts, nose caps and leading edges in space craft and hypersonic vehicles [3]. Research is being carried out to use HfB_2 to coat SiC and carbon in order to improve their high temperature oxidation resistance and ablation resistance in a range of aerospace applications. However, with HfB_2 being expensive, its commercialization in the aerospace industry has not proved feasible to date. It will therefore be attractive to find a convenient and cost effective method for the large scale synthesis of HfB_2 powder.

HfB_2 can be synthesized by various methods, including chemical routes, reactive processes and carbothermal reduction reactions. Chen et al. [3] synthesized nano sized hafnium diboride from $HfCl_4$ and $NaBH_4$ at 600°C using a hydrothermal reaction method. This is the lowest temperature reported for the synthesis of HfB_2 in the literature. Blum et al. [4] used a Hf and B powder mixture in a non self-propagating high-temperature synthesis (SHS) process to produce HfB_2 at 1500°C. They also reported a synthesis route employing metallic Hf strips and elemental boron powders. Despite the use of elements, the authors reported the presence of a significant level of unaccounted impurities that may or may not have been core shell structures of Hf and B. Hafnium diboride has also been prepared by the self-propagating high-temperature synthesis (SHS) route by Munir et al. [5]. These methods are expensive to scale up however, due to the high pressures or high temperatures involved. The solution derived precursor routes involving carbo/borothermal reduction reactions are reported to be the cheapest and most scalable processes for group IVB diborides, including HfB_2 [2]. Ni et al. [6] used excess B_4C and carbon to reduce HfO_2 at 1500-1600°C and obtained <1 µm HfB_2 powder. Equiaxed HfB_2 particles with particle sizes ranging between 1 – 1.5 µm were synthesized through borothermal reduction reactions at 1600°C by Guo-Jun Zhang et al. [7]. The current paper reports a sol-gel based synthesis route for HfB_2 powders at 1300°C. The sol-gel process was chosen as it forms a more homogeneous mixture and transforms to HfB_2 at lower temperatures than other approaches [8]. The method can also be favourable for commercialisation of HfB_2 nanopowder [9] and is suitable to produce ultra-high temperature ceramic (UHTC) coatings on carbon and SiC fibres [10]. A sol-gel mixture of hafnium chloride ($HfCl_4$), boric acid (H_3BO_3) and phenolic resin were used to obtain intimately mixed yet unreacted HfO_2, B_2O_3 and C that is then calcined. Usually this approach results in minor impurities such as HfO_2, HfC and B_4C; in this study we have optimised the ratios of the different precursors used to obtain HfB_2 with negligible impurities. The mechanism underpinning the formation of HfB_2 is also discussed as is the effect of varying the stoichiometries of B and C with respect to Hf on the structure of the resultant products.

2. Experimental

Hafnium (IV) chloride, $HfCl_4$, (98% purity, Sigma-Aldrich Company Ltd, Dorset, UK) was used as the hafnium source. A phenolic resin with a char yield of 51% was used as the carbon source (Cellobond J2027L, Momentive Speciality Chemicals, Louisville, USA). Boric acid, H_3BO_3 (99.5% purity, Fischer Scientific, Loughborough, UK) was the primary source of boron, with the exception of a few specified experiments where amorphous boron powder (95-97% purity, Sigma-Aldrich Company Ltd, Dorset, UK); was used. Ethanol (96% purity, Fischer Scientific, Loughborough, UK) was used as the solvent.

The basic reaction is shown by equation (1) and a flowchart for the synthesis is shown in Figure 1.

$$HfO_2 + B_2O_3 + 5C \rightarrow HfB_2 + 5CO\uparrow \quad (1a)$$

or

$$HfO_2 + 2B + 2C \rightarrow HfB_2 + 2CO\uparrow \quad (1b)$$

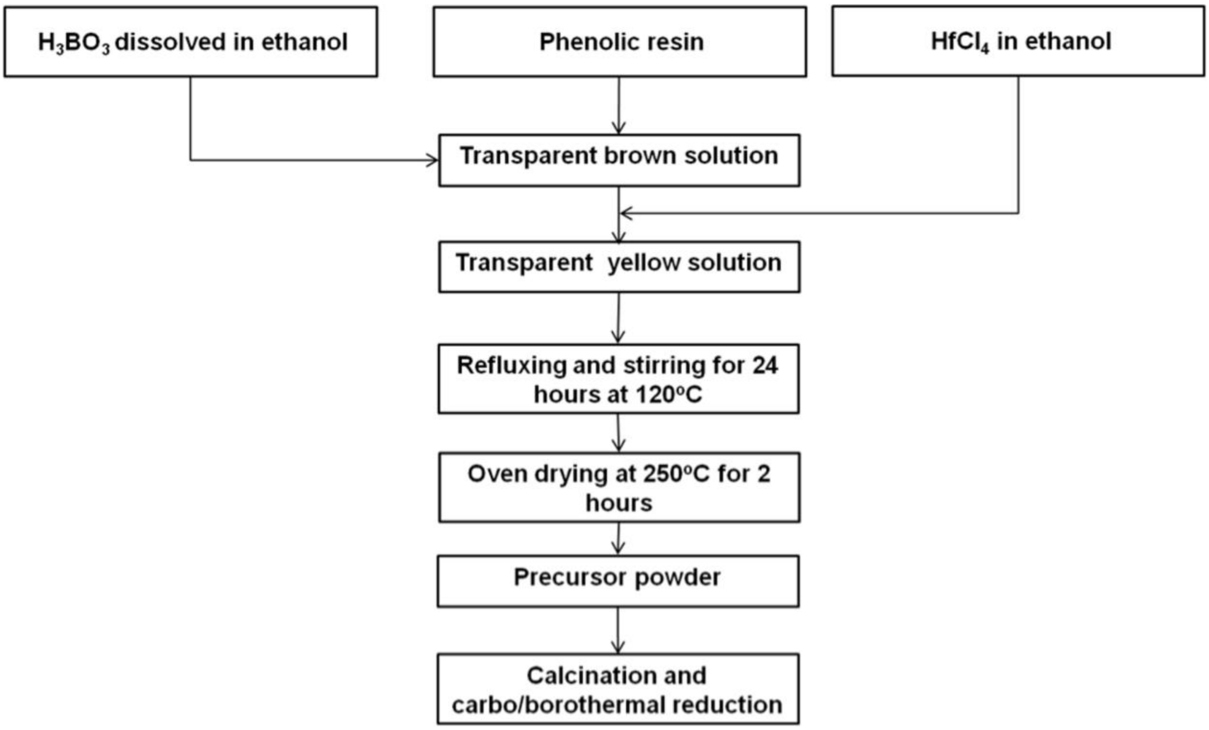

Figure 1: Flowchart for HfB_2 synthesis

The process involved the initial dissolution of H_3BO_3 in ethanol at 120°C followed by adding the appropriate amounts of $HfCl_4$ and phenolic resin, Table 1 [ii]. The stoichiometry of the reactants was varied to study their influence on the purity of HfB_2 powder. The solution mixture was stirred at 120°C for 24 hours with continuous refluxing to obtain a sol. The latter was dried at 250°C for two hours and ground to obtain the HfB_2 precursor powder.

The precursor powders were characterized using Fourier transform infrared spectroscopy (FTIR 8400S, Shimadzu, Maryland, USA), and thermo gravimetric analysis (TGA) coupled with differential scanning calorimetric analysis (DTA) (Netzch TGA/DSC, Germany). The TGA/DTA were run at temperatures up to 1600°C in an argon atmosphere. The heating rates were maintained at 5°C min^{-1} up to 1000°C and 3°C min^{-1} above 1000°C.

[ii] According to reaction 1, the stoichiometry of the Hf:B:C should be 1:2:5, but excess boron was added to account for the loss that occurs during high temperature heat treatments[7].

Table 1: Compositions investigated for HfB_2 synthesis

Sample	Elemental stoichiometry			Remarks
	Hf	B	C	
HBC	1	2	5	Exact stoichiometry, as equation 1a
HB_eC	1	3 – 3.8	5	Equation 1a with slight excess B to compensate for losses
HBC_e	1	3	10	Equation 1a with excess C
HB_eC_e	1	6	10	Equation 1a with excess B and C
HB	1	3	0	Equation 1a without C
HB_aC	1	2	2	Equation 1b using amorphous B powder
B_eC_e	0	6	10	Equation 1a without Hf; attempt to synthesize B_4C
HC	1	0	3	Attempt to synthesize HfC

The carbo/borothermal reduction reaction was carried out in an argon atmosphere at temperatures in the range 1300 – 1600^oC in a horizontal tube furnace (TSH17/75/450, Elite Thermal Systems Ltd, UK) fitted with a 99.7% pure alumina tube. The heating and cooling rates were maintained at 5^oC min^{-1} up to 1000^oC and 3^oC min^{-1} above 1000^oC in all cases. An argon – 1% hydrogen mixture was passed through the tube for the first 500°C for all of the runs. This helped to remove both the Cl^- ions [11] trapped in the system as HCl vapours[iii] and also the oxygen from the tube. An estimation of the particle size of the powders was obtained using field emission gun scanning electron microscopy (FEGSEM 1530 VP, Carl Zeiss (Leo), Oberkochen, Germany). Phase analysis of the powders was carried out by transmission electron microscope (TEM 100 CX, JEOL JEM, Munich, Germany) in diffraction mode and by room temperature XRD using Cu Kα radiation (Bruker D8 X-Ray Diffractometer, Bruker, Coventry, UK). The d spacings were calculated from the 2θ values and were compared with the standard values from the JCPDS powder diffraction files to identify the phases. The percentage of carbon content in the powders was also analysed (CE-440 Elemental Analyser, Exeter Analytical Inc., Coventry, UK). A Focused dual ion beam (FIB – FEI Nova 600 Nanolab Dual Beam system, Eindhoven, The Netherlands) was used to prepare the sample for electron backscattered diffraction (EBSD) imaging (Hikari hi-speed camera fitted with the FIB). Thermodynamic calculations were carried out using Factsage 6.1 (CRCT-ThermFact Inc. Canada & GTT-Technologies, Germany).

3. Results and Discussion

3.1. Powder Synthesis

The FTIR absorption spectra for all the HfB_2 precursors formed with different Hf:C:B molar ratios and dried at 250°C for 2 hours were very similar; one of the spectra across the 4000 – 400 cm^{-1} range is shown in Figure 2. The broad peak at around 3400 cm^{-1} is attributed to the O-H stretching vibrations associated with the hydroxyl

---

[iii] $HfCl_4$ being highly hygroscopic and oxygen sensitive reacts with moisture in both the air and the ethanol during the synthesis stage to release HCl vapours. Any reaction with H_2 gas only triggers this reaction and helps remove Cl^- ions from the precursor powder.

groups in the phenolic resin, boric acid and the Hf-OH stretching vibrations. The peaks at 418, 1392, 2841 and 2914 cm^{-1} are attributed to the aliphatic C-H stretching vibrations from the phenolic resin, whilst those at 543, 1099 and 1622 cm^{-1} represent the aromatic C-H deformation and C=C deformation from the phenolic resin. The peaks at 2330 and 2357 cm^{-1} are due to C=O stretching arising from the CO_2 and $C_3O_2^+$ groups present in the system. The O-B-O stretching vibrations peaks are present at 449, 520 and 675 cm^{-1} and these are associated with boric acid present in the system. The peaks at 642 and 748 cm^{-1} are attributed to the OHfO- asymmetric stretching [12]. The FTIR result confirms that there was no complex formation between the reactants and that at the end of the sol-gel process and subsequent drying step, the precursor powder consisted of H_3BO_3, $Hf(OH)_4$ and aromatic and aliphatic chains resulting from the cross-linking of the phenolic resin.

Figure 3 shows the TGA/DSC curves of the precursor powder HB_eC. TG analysis shows that the main weight loss occurred below 700^{o}C due to the evaporation of the bound water and the decomposition of the phenolic resin and evolution of chlorides. After 1275^{o}C, there was further weight loss up to 1600^{o}C due to the onset of the carbo/borothermal reduction reaction, which is also indicated by the endothermic peak at 1275^{o}C in the DSC curve. The maximum weight loss was 51 wt%.

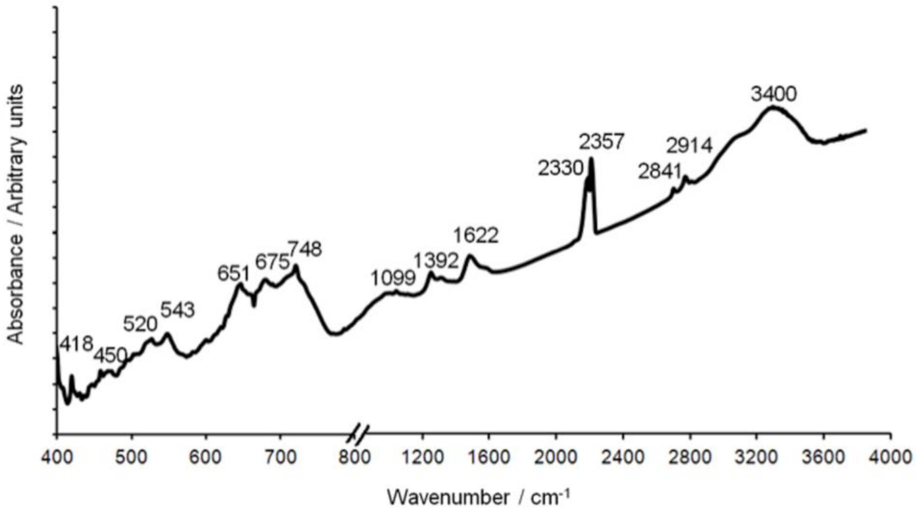

Figure 2: FTIR of precursor powder HBC

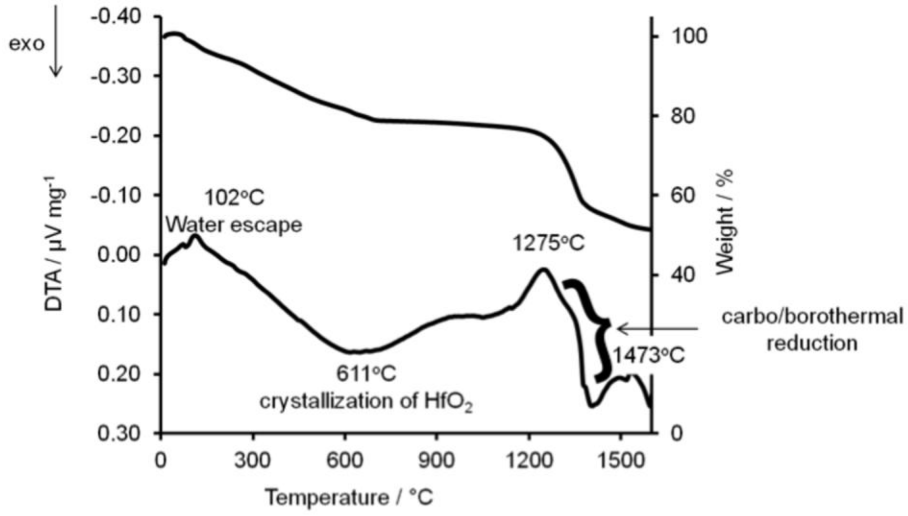

Figure 3: TGA/DSC of precursor powder HB$_e$C

Figure 4 shows the XRD patterns for the HB$_e$C precursor powders heated from 600^{o}C to 1500^{o}C with a 0.1 h dwell. The results show that HfO$_2$ was formed at 650^{o}C. At this temperature, the degradation of phenolic resin to carbon and dehydration of boric acid to boron trioxide will also have been complete [13]. Therefore, at 650^{o}C the powder mixture consisted of un-reacted but intimately mixed B$_2$O$_3$, HfO$_2$ and C. By 1300^{o}C HfB$_2$ peaks formed, indicating the onset formation of HfB$_2$ which is in support of the TGA/DSC results in Figure 3, where the endothermic peak appeared at 1275°C.

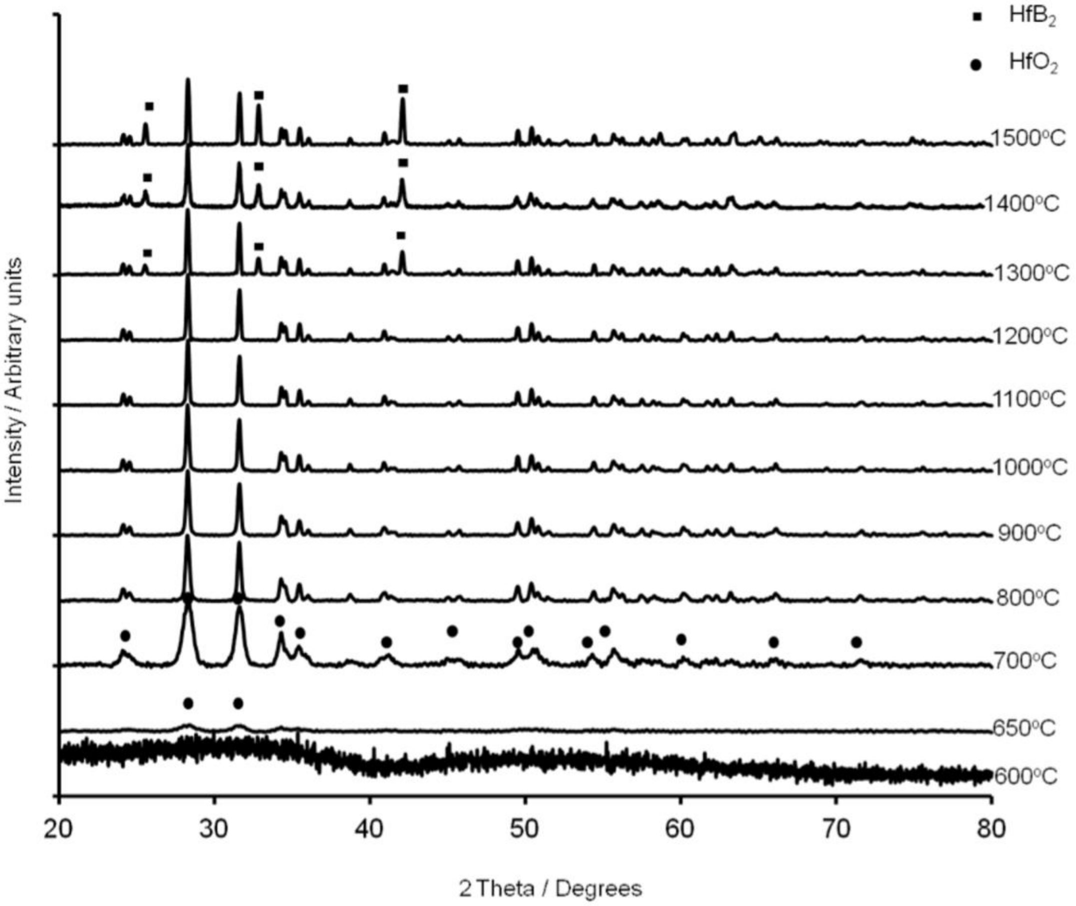

Figure 4: XRD patterns of the HB_eC precursor powder heated from 600°C to 1500°C with a 0.1 h dwell

Figure 5 shows the indexed XRD patterns of HBC and HB_eC calcined at 1600°C for 2 h. The patterns were indexed according to the JCPDS cards 00-039-1491 and 00-038-1398 for HfC and HfB_2 respectively. It can be seen that the pattern corresponding to the HBC precursor, which was made using the stoichiometric mix of the 3 elements, includes significant amounts of HfC impurity, whilst the HB_eC XRD pattern shows only HfB_2 peaks. This confirms the need to include excess B in the initial mix to allow for B_2O_3 losses by vaporization, as observed by Ni et al.[6]. The boron loss depended on various factors like humidity, flow rate of the inert gases, and substrate used. For this reason the ratio of B:Hf was kept between 3:1 and 3.8:1 instead of 2:1 for subsequent compositions.

Both isothermal TGA and subsequent heat treatment in the tube furnace revealed that 25 h was needed at 1300°C to complete the carbo/borothermal reaction and achieve hexagonal HfB_2 with no secondary phases, Figure 6; only 2 h was required at 1600°C.

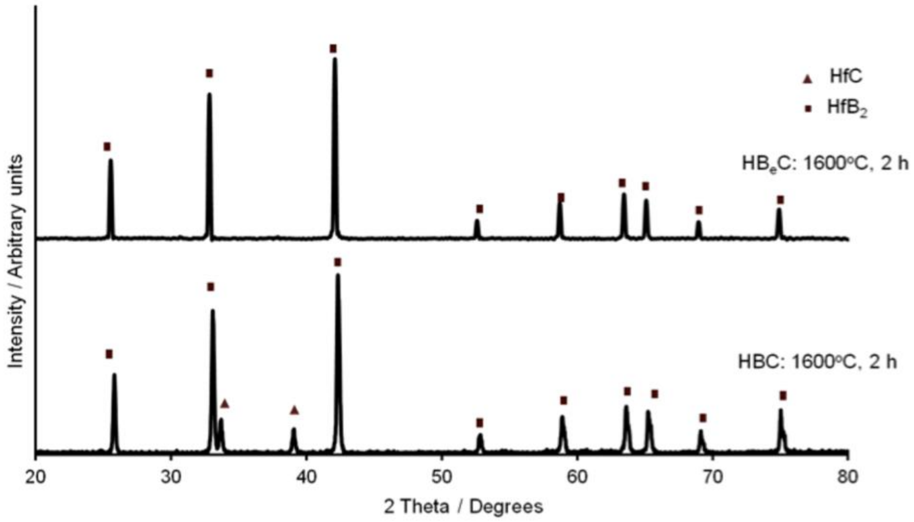

Figure 5: XRD patterns of the HBC and HB_eC precursor powders calcined at 1600°C for 2 h

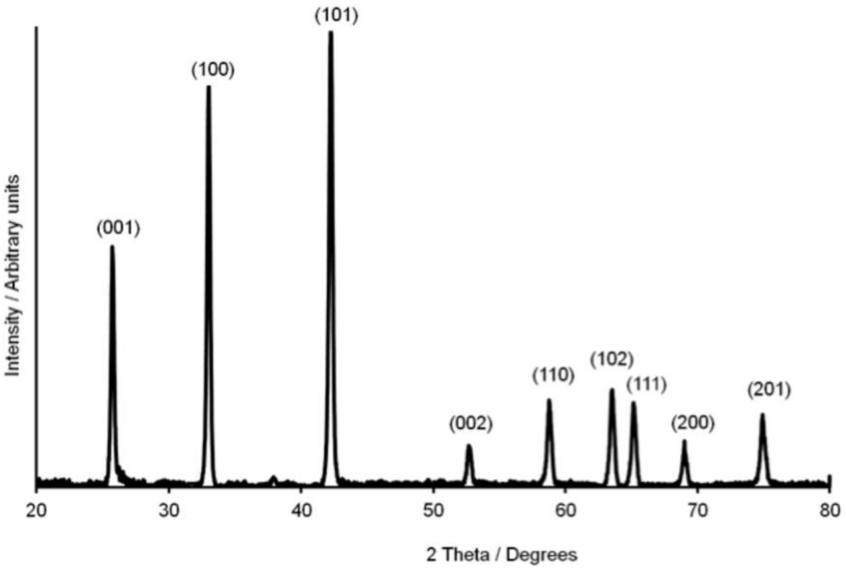

Figure 6: XRD of HB_eC precursor powder calcined at 1300°C for 25 h

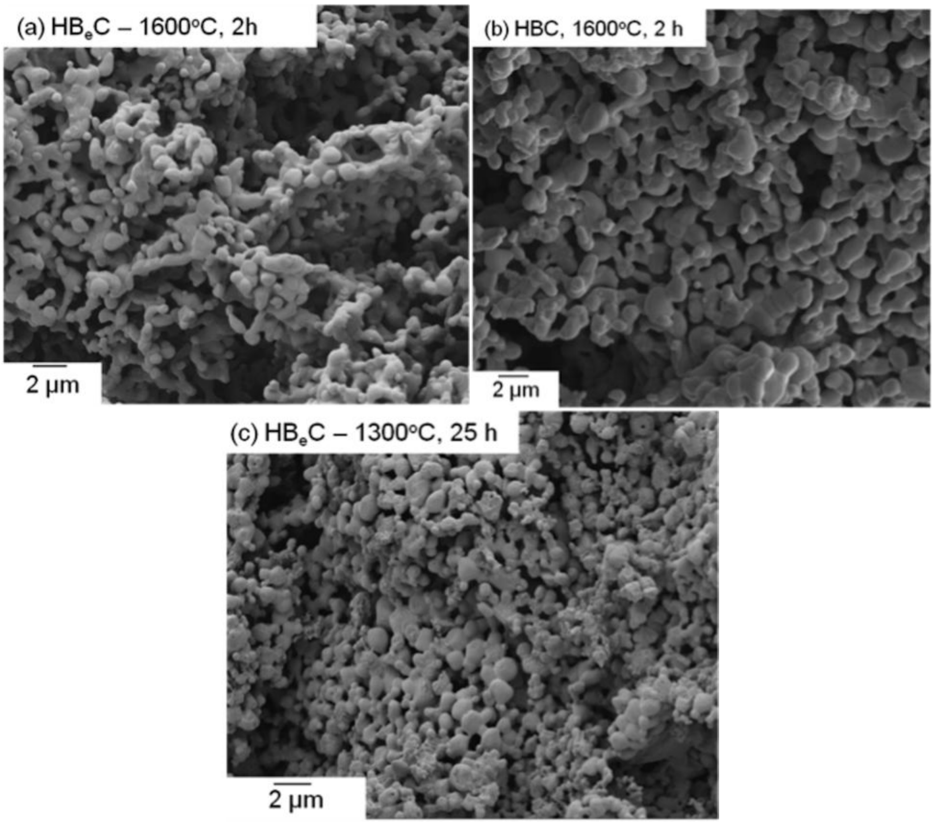

Figure 7: FEGSEM micrographs showing the particle morphology for (a) HB_eC, (b) HBC, calcined at 1600°C for 2 h (c) HB_eC calcined at 1300°C for 25 h

As seen from Figure 7, the products from HB_eC and HBC have a very similar particle size of about 1 – 2 µm indicating that an increase in boron oxide content does not have any effect on the particle size of the end product. On the other hand, lowering the synthesis temperature from 1600°C to 1300°C and increasing the dwell time from 2 to 25 h had the effect of slightly decreasing the particle size, the size of the particles obtained from HB_eC ranged from 0.25 – 2 µm, but also yielded a high proportion of rod shaped particles, Figure 8a. It is believed that the particles grow into rods due to the long heating time involved with the growth occurring along the c-axis, Figure 8b. Similar structures were reported by Begin et al. [14] when they synthesized HfB_2 through mechanical activation. The percentage of carbon in this powder, as determined by elemental CHN analysis, was around 0.19%.

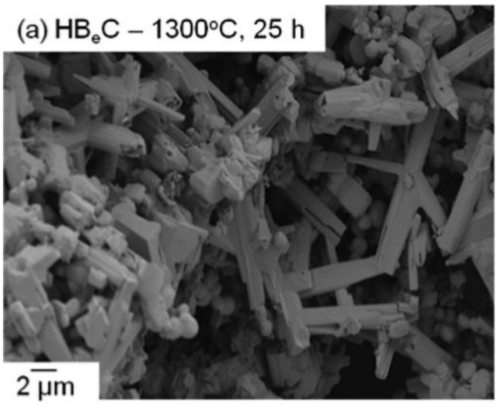
(a) HB_eC – 1300°C, 25 h

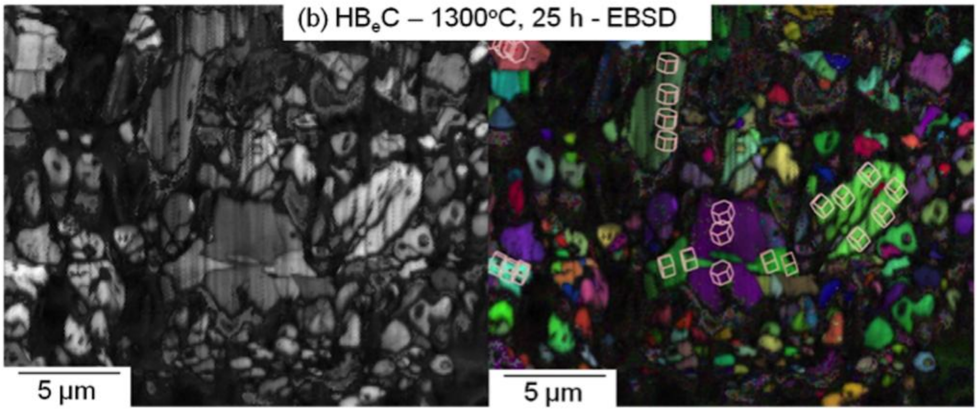
(b) HB_eC – 1300°C, 25 h - EBSD

Figure 8: a) FEGSEM of HB_eC calcined at 1300°C for 25 h showing rod shaped particles, b) FIB and EBSD image of 'a'

3.2. Effect of Varying the Hf:B and Hf:C molar ratio

No HfB_2 formation was observed after heat treating HB to 1600°C for 5 h; the end product consisted of HfO_2 and B_2O_3, Figure 9(a); as identified by EDX. This confirms that, without carbon, no reduction reaction occurs in the system, i.e. carbon plays an important role in creating the reducing conditions required for HfB_2 formation. In the presence of excess carbon, HBC_e, the end product contained both HfB_2 and ~0.19%, free carbon, as determined by elemental CHN analysis, Figure 9(b). Interestingly, the size of the HfB_2 particles was only 20 – 30 nm. On the other hand, if both excess boron and carbon were used, HB_eC_e, then boron carbide was formed, Figure 9(c) and the HfB_2 particles were 1 – 2 µm in size. The presence of the free carbon in the HBC_e system thus appears to act as a barrier, preventing particle growth and yielding much finer HfB_2 compared to the other powders synthesised, though attempts to remove the residual carbon without chemically degrading the nano HfB_2 failed. Without free carbon, the particles are free to grow in size during calcination. Similar results were reported by Krishnarao et. al. [15] during TiB_2 synthesis. Reactions 2 and 3 represent the excess C and B scenarios respectively:

With excess carbon

$$HfO_2 + B_2O_3 + (5+x)C \rightarrow HfO_2 + 2B + (2+x)C + 3CO\uparrow \rightarrow HfB_2 + xC + 2CO\uparrow \qquad (2)$$

With excess boron

$$HfO_2 + 3B_2O_3 + (5+x)C \rightarrow HfO_2 + 6B + (x-4)C + 9CO\uparrow \rightarrow HfB_2 + {}^{1}/_{3}(12B(C\text{-}B\text{-}C)) + 2CO\uparrow \qquad (3)$$

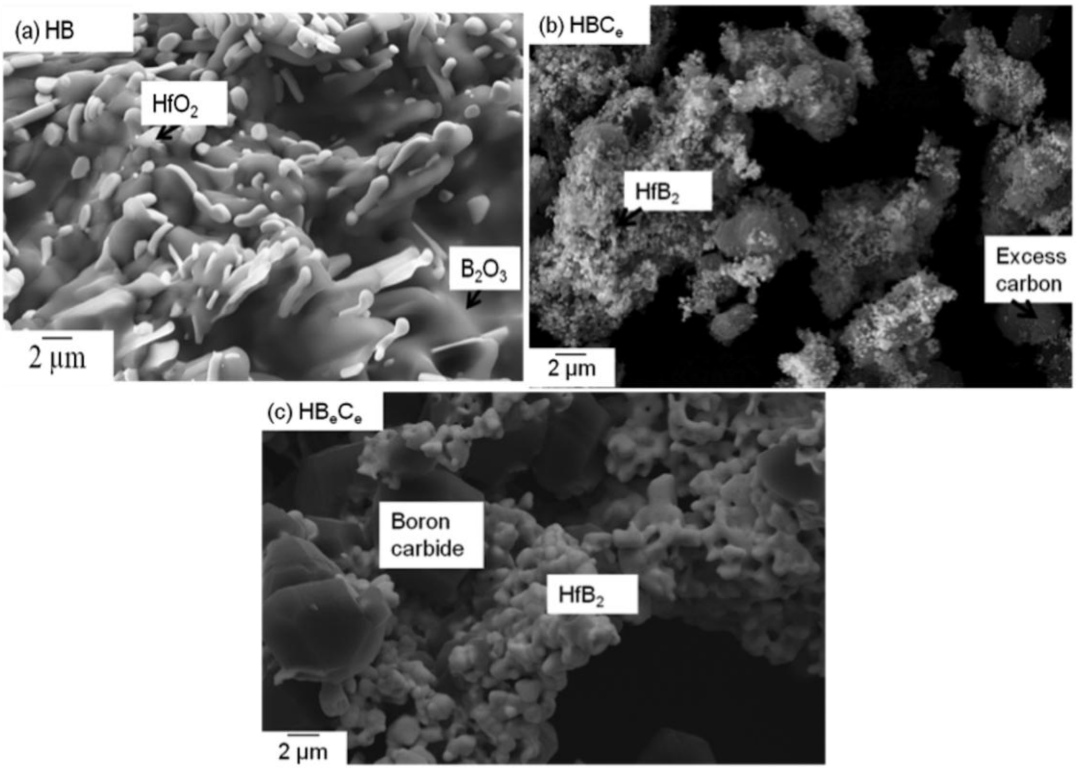

Figure 9: (a) HB, (b) HBC_e and (c) HB_eC_e precursor powders, all calcined at 1600°C for 2 h

3.3. Reaction Mechanism

For any reaction to be thermodynamically favourable and spontaneous the Gibbs free energy (ΔG) of the reaction should be negative. For reaction 1a,

$$HfO_2 + B_2O_3 + 5C \rightarrow HfB_2 + 5CO\uparrow$$

ΔG is negative only at >1523°C, as calculated using Factsage 6.1, however, it has been shown that HfB_2 forms at a temperature as low as 1300°C. In order to explain this difference the mechanism by which HfO_2, B_2O_3 and C react to form HfB_2 was studied in detail.

There are three possible routes by which these three reactants could form HfB_2; they are indicated below as reactions 4, 5 and 6. Note that the latter has some variations within it.

$$HfO_2 + B_2O_3 + 5C \rightarrow HfC + B_2O_3 + 3C + 2CO\uparrow \rightarrow HfB_2 + 3CO\uparrow \tag{4}$$

$$HfO_2 + B_2O_3 + 5C \rightarrow HfO_2 + ½B_4C + 1.5C + 3CO\uparrow \rightarrow HfB_2 + 2CO\uparrow \tag{5}$$

$$HfO_2 + B_2O_3 + 5C \rightarrow HfO_2 + 2B \text{ or } B_2O_2 + 2C \text{ or } 4C + 3CO \text{ or } CO\uparrow \rightarrow HfB_2 + 2CO \text{ or } 4CO\uparrow \tag{6}$$

The intermediate reactions 4i, 5i and 6i are given below along with their ΔG values.

$$HfC + B_2O_3 + 3C \rightarrow HfB_2 + 3CO\uparrow \qquad \Delta G < 0 \text{ above } 1425^oC \tag{4i}$$

$$HfO_2 + ½B_4C + 1.5C \rightarrow HfB_2 + 2CO\uparrow \qquad \Delta G < 0 \text{ above } 1453^oC \tag{5i}$$

$$HfO_2 + 2B \text{ or } B_2O_2 + 2C \text{ or } 4C \rightarrow HfB_2 + 2CO \text{ or } 4CO\uparrow \qquad \Delta G < 0 \text{ above } 1350^oC \tag{6i}$$

Hence, based on thermodynamic calculations, the only reaction that has a realistic chance of leading to HfB_2 formation at ~1300^oC is reaction 6. Note that at higher temperatures, e.g. above ~1450^oC, there may be more than one reaction path.

If the mechanism of formation of HfB_2 were to proceed through reaction 4, then HfC should form at a much lower temperature than HfB_2. From Figure 4 it can be seen that HfC peaks did not appear even by 1500^oC, though in theory this could be due to the HfC being consumed immediately as it is formed. To understand this better precursor powder HC, made from Hf and C sources, was prepared and heated from 600^oC to 1500^oC with 0.1 h dwell and subjected to XRD analysis. As seen from Figure 10, HfO_2 formation occurred at 650^oC, Figure 4, but HfC peaks only began to appear at 1500^oC. Blum et al. [16] observed that there was a kinetic preference and a lower threshold temperature for the onset of the reaction of Hf with B powder compared to the reaction with C powder. The present work shows that the same also occurs for the reaction between HfO_2 and B or C. Hence it is concluded that HfC is not an intermediate product during HfB_2 synthesis, suggesting that reaction 4 is not the correct formation mechanism.

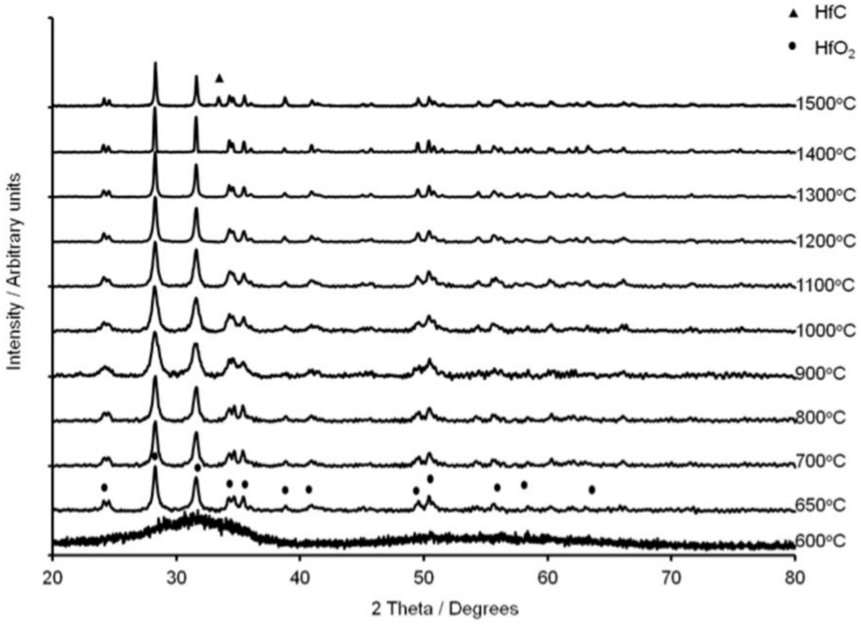

Figure 10: XRD patterns of the HC precursor powder heated from 600^{o}C to 1500^{o}C with a 0.1 h dwell

When the HB_eC_e precursor powder was calcined there was clear evidence of HfB_2 formation at 1300^{o}C, as for the HB_eC. However, although no boron carbide phases were detected by XRD, even after heat treatment at 1600^{o}C for 2 hours, Figure 11, it was detected by electron microscopy, Figure 9c, and EDX analysis revealed the presence of both boron and carbon in the faceted phase. The amount of the boron carbide phase was probably below the level for XRD detection, especially given the low X-ray density of boron carbide in comparison with hafnium-based compounds.

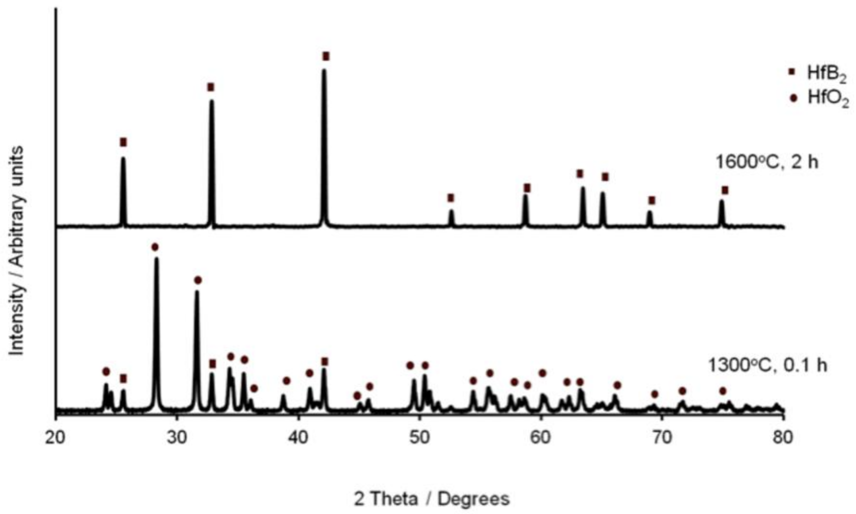

Figure 11: XRD of the HB_eC_e precursor powder calcined at 1300°C for 0.1 h and 1600°C for 2 h

Reaction 5 requires that carbon reacts with B_2O_3 to form B_4C as an intermediate product, which subsequently reacts with HfO_2 to form HfB_2. If this is the case then B_4C has to form below 1300°C, i.e., at a temperature lower than that required for HfB_2 formation. Since potential boron phases were not detected by XRD when they occurred in combination with a heavy metal compound, a composition containing only boron and carbon was synthesized (B_eC_e). The carbothermic reduction sequence of B_2O_3 is presented by reactions 7, 8, 9 and 10 [17,18].

$$B_2O_3 + C \rightarrow B_2O_2 + CO\uparrow \quad (7)$$

$$B_2O_2 + C \rightarrow B_2O + CO\uparrow \quad (8)$$

$$B_2O + C \rightarrow 2B + CO\uparrow \quad (9)$$

$$4B + C \rightarrow B_4C \quad (10)$$

Figure 12 shows the XRD pattern of the B_eC_e precursor powder calcined at different temperatures in a scan range of $2\theta = 30^o - 40^o$. It is evident that a boron carbide peak does not appear until 1450^oC and hence it is very unlikely to be an intermediate product in HfB_2 formation, unless there are some very significant, and unknown, catalytic effects occurring when Hf-based compounds are present.

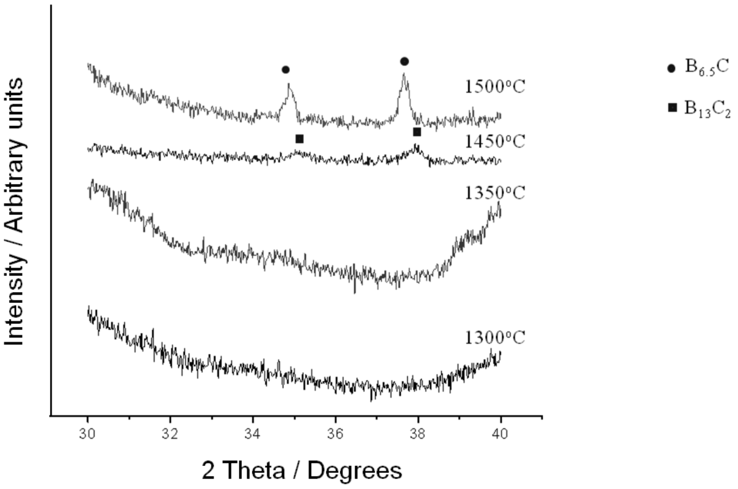

Figure 12: XRD patterns of the B_eC_e precursor calcined at different temperatures for 0.1 h

This may possibly suggest that, at the end of reactions 7, 8 and 9, the products react with HfO_2 to form HfB_2 before reaction 10 can occur. This is the basis of reaction 6, according to which HfB_2 is formed by the reaction between HfO_2 and boron sub oxides and/or amorphous boron. Due to the limitations of experimental conditions it was difficult to detect B_2O_2, B_2O or amorphous B in the intermediate reaction products. Hence, to shed further light on the issue, the experiments were performed involving amorphous boron powder as the source of boron.

High temperature DSC curves for the precursors HB_eC and HB_aC, showed similar trends, Figure 13. The total weight loss for HB_aC was 34 wt% whilst that for HB_eC was 51 wt%, as mentioned earlier. The difference in the total weight loss may be due to the loss of B_2O_3 in the HB_eC system. The weight loss for the HB_aC system occurred up to 500^oC due to the loss of physisorbed and chemisorbed water and degradation of the phenolic resin, whilst that for HB_eC occurred up to 700°C due to the presence of B_2O_3 and excess resin. The weight losses remained stable up to 1275°C in both cases and then rapidly decreased and stabilised towards 1600°C.

The endothermic peaks depicting the carbo/borothermal reduction reactions at 1275°C and 1470°C are identical for both precursor powders, indicating that the reaction paths were similar for the two. This could only mean that either the B_2O_3 had dissociated into B during the course of the HfB_2 formation in the HB_eC precursor powder or the amorphous B in the HB_aC precursor had oxidised into B_2O_3. Since the reaction was carried out in a reducing atmosphere in the presence of carbon, the likelihood for the latter is extremely small.

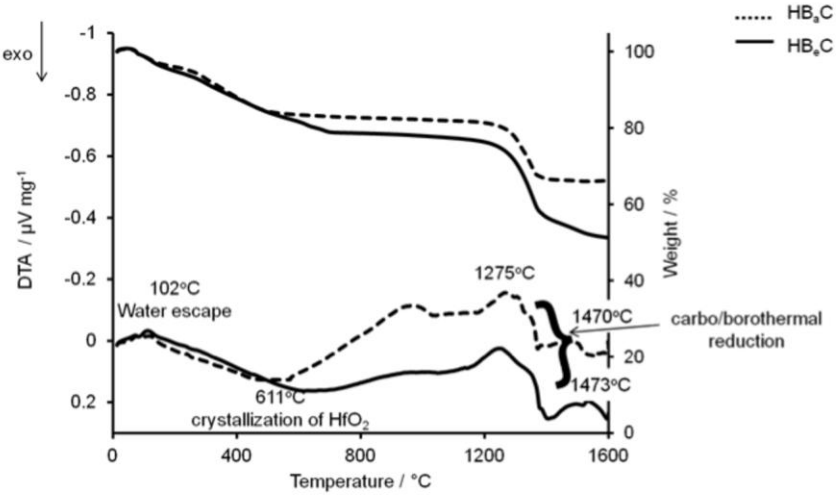

Figure 13: TGA/DSC of HB_eC and HB_aC precursor powders

This result, combined with the Gibbs free energy value, indicates that the formation of HfB_2 at 1300°C is most likely to occur through the formation of amorphous boron or boron sub oxides as the intermediate product (Reaction 6), though, as indicated earlier, at higher temperatures there could be more than one reaction mechanism taking place simultaneously.

4. Conclusions

HfB_2 powder has been prepared using a simple sol-gel approach. The ratio of Hf:B:C required for achieving this purity was 1:3-3.8:5. The effect of changing the stoichiometry of the precursors on the purity of the final powders was studied. If the carbon source was in excess then the final product contained free carbon whilst if the both boron (Hf:B $\geq$ 6) and carbon source were in excess then the final product consisted of boron carbide in addition to the HfB_2 particles. If free carbon was present in the system, it acted as a capping agent for the HfB_2 particles and lead to a much finer final particle size. However, it was not possible to remove the carbon without degrading the HfB_2. Calcination temperatures as low as 1300^{o}C could be used to form HfB_2, however it required 25 h to form the pure phase. This long dwell time gave rise to a significant fraction of rod shaped particles, with growth occurring along the c-axis.

During carbo/borothermal reduction, the formation of HfB_2 occurred before HfC and B_4C formation, so it was concluded that neither HfC nor B_4C were the intermediates. The TGA/DSC results of the HfB_2 precursor powders made from B_2O_3 and amorphous B, however, showed identical peaks for the carbo/borothermal reduction reactions and hence it is believed that the only thermodynamically favourable path for HfO_2, B_2O_3 and C to react and form HfB_2 at 1300^{o}C is through the intermediate formation of amorphous B or boron sub oxides (reaction 6), although at higher temperatures more than one reaction mechanism could be active.

Acknowledgement

The authors would like to thank Dr Luc Vandeperre, senior lecturer at Imperial College, London for help with thermodynamic calculations and for analysing our samples using high temperature TGA/DSC analysis.

References

[1] Opeka MM, Talmy IG and Zaykoski JA. J. Mater. Sci 2004;39:5887–904.

[2] Fahrenholtz WG and Hilmas GE. J. Am. Ceram. Soc 2007;90(5):1347–64.

[3] Chen L, Gu Y, Shi L, Yang Z, Ma J and Qian Y. J. Alloys Compd 2004;368(2):353–6.

[4] Blum YD, Marschall J, Hui D, Adair B and Vestel M. J. Am. Ceram. Soc 2008;91(5):1481–88.

[5] Munir ZA. Metall. Trans. A 1992;23(1):7-13.

[6] Ni DW, Zhang GJ, Kan YM and Wang PL. J. Am. Ceram. Soc 2008;91(8):2709-12.

[7] Zhang GJ, Guo WM, Ni DW and Kan YM. J.Phys. Conf. Ser 2009; 176(1):1742-6596.

[8] Yan Y, Huang Z, Dong S and Jiang D. J. Am. Ceram. Soc 2006;89(11):3585-8.

[9] Sacks MD, Wang C, Yang Z and Jain A. J. Mater. Sci 2004;39:6057–66.

[10] Venugopal S, Paul A, Vaidhyanathan B, Binner J, Heaton A and Brown P. Ceram. Eng. Sci. Proc 201;32:151-60.

[11] Wunder VK, Popovska N and Emig G. Electrochem. Soc. Proc 1999;98(23):263–7.

[12] www.webbook.nist.gov

[13] Parsons J and Milberg ME. J. Am. Ceram. Soc 1960;43(6):326–30.

[14] Bégin-Colin S, Le Caër G, Barraud E and Humbert O. J. Mater. Sci 2004;39(16–17):5081–9.

[15] Krishnarao RV and Subrahmanyam J. Mater. Sci. Eng A 2003;362:145-51.

[16] Blum YD, Marschall J, Hui D, Adair B and Vestel M. J. Am. Ceram. Soc 2008;91:1481–8.

[17] Bigdeloo JA and Hadian AM. Int. J. Recent Trends Eng 2009;1(5):176-80.

[18] Dacic BZ, Jokanovic V, Jokanovic B and Dramicanin MD. J. Alloys Compd 2006;413:198–205.